Journal of Biomedical Optics

SPIEDigitalLibrary.org/jbo

Correlation of visually evoked intrinsic optical signals and electroretinograms recorded from chicken retina with a combined functional optical coherence tomography and electroretinography system

Alireza Akhlagh Moayed
Sepideh Hariri
Vivian Choh
Kostadinka Bizheva

SPIE

Correlation of visually evoked intrinsic optical signals and electroretinograms recorded from chicken retina with a combined functional optical coherence tomography and electroretinography system

Alireza Akhlagh Moayed,[a] Sepideh Hariri,[a] Vivian Choh,[b] and Kostadinka Bizheva[a]
[a]University of Waterloo, Department of Physics and Astronomy, 200 University Avenue West, Waterloo, Ontario N2L3G1, Canada
[b]School of Optometry, University of Waterloo, 200 University Avenue West, Waterloo, Ontario N2L 3G1, Canada

Abstract. Visually evoked fast intrinsic optical signals (IOSs) were recorded for the first time *in vivo* from all layers of healthy chicken retina by using a combined functional optical coherence tomography (fOCT) and electroretinography (ERG) system. The fast IOSs were observed to develop within ~5 ms from the on-set of the visual stimulus, whereas slow IOSs were measured up to 1 s later. The visually evoked IOSs and ERG traces were recorded simultaneously, and a clear correlation was observed between them. The ability to measure visually evoked fast IOSs non-invasively and *in vivo* from individual retinal layers could significantly improve the understanding of the complex communication between different retinal cell types in healthy and diseased retinas. [DOI: 10.1117/1.JBO.17.1.016011]

Keywords: Optical coherence tomography; *in vivo*; imaging; retina; functional imaging; electroretinography.

Paper 11444L received Aug. 16, 2011; revised manuscript received Nov. 16, 2011; accepted for publication Nov. 17, 2011; published online Feb. 8, 2012.

1 Introduction

The retina is a highly organized neural tissue in which retinal neurons and other cells form a well-defined, layered structure. Understanding the communication between retinal cells in healthy and diseased retinas and correlating retinal structure with function have been the goals of many studies. The main method used in clinical evaluation of retinal function is electroretinography[1] (ERG), a technique that records the electrical activity of visually stimulated retinas. Because ERG records an integrated response from all retinal layers to external stimulation, direct correlation between the cellular retinal structure and function is not trivial.

Because the optical reflectivity of neural tissue changes with external stimulation,[2,3] various optical techniques, such as fundus reflectance, near-infrared microscopy, confocal microscopy, and adaptive optics, have been utilized to measure visually evoked intrinsic optical signals (IOSs) in the retina.[4–10] Fast IOSs, which develop within ~50 ms from the stimulus onset, were measured in individual retinal layers *ex vivo*[10] using near-infrared microscopy; however, there are no published records of similar recordings *in vivo*. Optical coherence tomography (OCT) is an imaging technique that allows for noninvasive, *in vivo*, high-resolution imaging of the layered structure of the retina.[11] Functional OCT (fOCT) was recently introduced as a novel technique for noninvasive probing of retinal function of individual retinal layers in *ex vivo* retinal preparations,[12,13] *in vivo*animal models,[14] and healthy human subjects.[15–17]

Here in we present, to the best of our knowledge, the first *in vivo* recordings of fast visually evoked IOSs from individual retinal layers measured by fOCT.

2 Methods

In this study, we utilized a combined fOCT-ERG system that was recently developed by our research group.[18] Briefly, the fOCT system is based on spectral domain OCT technology and is designed to operate in the 1,060 nm wavelength range. This spectral region was chosen to ensure no visual stimulation of the retinal photoreceptors by the imaging beam. The fOCT system provides ~3.5 μm axial and ~5 μm lateral resolution in the chicken retina, a line rate of 22 μs and SNR of ~95 dB for 1.3-mW power of the imaging beam at the cornea. The fOCT system's data acquisition was synchronized with that of a commercial ERG system (Diagnosys LLC, Lowell, MA, USA). A custom-designed visual stimulator integrated with the optical imaging probe and described in detail in our earlier publication[18] was used to project a ~2 mm diameter spot on the retinal surface with preselected color, duration, and intensity of the visual stimulus.

Five 13-days-old White Leghorn chickens (*Gallus domesticus*) were used in this study. The chicken retina was selected as an animal model because it is cone-dominated and devoid of intraretinal vasculature that could create shadows and potentially interfere with the IOS measurements from different retinal layers. The imaging procedure we used was approved by the University of Waterloo Animal Research Ethics Committee. Chickens were dark-adapted for 1 h in a lightproof box and then anesthetized with 1.5% isoflurane. The animals were then placed in a custom holder to restrain head motion during

Address all correspondence to: Kostadinka Bizheva, Department of Physics and Astronomy, University of Waterloo, 200 University Avenue West, Waterloo, Canada, ON N2L3G1. Tel: 519 888 4567 x37517; Fax: 519 746 8115; E-mail: kbizheva@uwaterloo.ca

0091-3286/2012/$25.00

the imaging procedure and allow for easy alignment of the eye with respect to the imaging beam. The imaging procedure was carried out in a dark Faraday cage, then placed in a dark room to prevent accidental ambient light exposure and minimize electromagnetic noise. A lid retractor was used to immobilize the lid of the chicken eye, and eye drops were administered frequently to hydrate the cornea. ERG recordings were acquired by placing a loop electrode on the cornea and ground and reference electrodes into the chicken's mouth and on the skin, respectively.

3 Results

Structural and functional images were acquired from the chicken retina. Figure 1(a) shows a representative morphological tomogram where all retinal layers are clearly resolved. The red dashed line marks a region in the retina from which visually evoked IOSs were measured. Functional OCT data were recorded by repeatedly scanning a ~120 μm-long strip of the retina located in the center of the visual stimulus spot. The width of the strip, determined by the diameter of the imaging beam, was estimated to be ~5 μm at the focal plane of the imaging beam. Each fOCT image [B-scan; Fig. 1(b)] corresponds to a single sweep over the retinal strip, consists of 250 A-scans, required ~7 ms of acquisition time (80/20 duty cycle), and represents one data point in the extracted, averaged IOS traces, a representative of which is shown in Fig. 1(c). Each fOCT recording consists of 225 B-scans for a total acquisition time of ~1.5 s. Two types of fOCT recordings were acquired from the same location in the retina in sequence: a baseline ("dark scan"), which was recorded in complete darkness and used as a reference, and a "single-flash" recording, in which a single green color flash of 7-ms duration and ~1.9 Cd/cm^2 intensity at the retinal surface was applied 500 ms after the start of the data acquisition. The fOCT recordings were repeated up to 10 times in the right eye of each bird, with 3 minpauses between consecutive fOCT recordings to allow for photoreceptor recovery.

The fOCT B-scans were aligned in 3D stacks[18] and processed with ImageJ software to correct for motion artefacts arising from involuntary eye motion and heart rate. Successive B-scans were cross-correlated to compensate for linear shifts in the x and z directions (along the imaged strip and the retinal depth, respectively) and for rotational misalignment. Up to one-third of the volume of each 3D image stack was removed in the x direction from the two ends of the imaged strip during the alignment procedure because of eye motion artefacts. The IOSs were calculated for each pixel of the 3D image matrix by averaging the intensity of each pixel over time for the first 500 ms (prestimulus) and subtracting the average from the entire fOCT recording for that pixel. The differential intensity data were then normalized to the prestimulus average intensity to calculate the fractional changes in the tissue optical reflectivity. To determine the visually evoked IOSs originating from each retinal layer, the fOCT B-scans were segmented manually [red lines in Fig. 1(b)], and the data were averaged in the z direction over the thickness of each segmented layer and in the x direction over the length of the B-scan (the length of the imaged strip of the retina). Because of its small size, low contrast, and high speckle noise issues, the ganglion cell layer (GCL) could not be segmented with high confidence from the nerve fiber layer (NFL); therefore, IOSs were calculated from the combined NFL and GCL. For the same reasons, the photoreceptor outer segments (OSs) and retinal pigmented epithelium (RPE), as well as the outer plexiform layer (OPL) and the outer nuclear layer (ONL), were also combined. Future development of more precise automatic layer segmentation algorithms may allow for separation of the functional responses observed in thin individual retinal layers. Representative IOS traces are shown in Fig. 1(c), where the black line corresponds to a "dark scan" and the red line to a "single flash" recording. The IOSs in Fig. 1(c) are statistical averages of six "dark" and six "single-flash" fOCT recordings from a single eye and represent the integrated retinal response to the visual stimulus from the NFL to the RPE. The thin yellow line marks the light flash onset and duration.

Representative IOS traces measured in individual segmented retinal layers are shown in Fig. 2. The black line corresponds to a "dark scan." The thin vertical yellow strip at 500 ms marks the onset and duration of the light stimulus flash. The gray area in Fig. 2 marks a 100-ms time period of interest that is magnified in Fig. 3 for easy comparison and analysis of the IOS data. The IOS recordings from all retinal layers showed fast increases and/or decreases of the tissue reflectivity within ~80 ms from the visual stimulus onset (fast IOSs represented by gray area in Fig. 2) and slow variation of the optical changes for the rest of

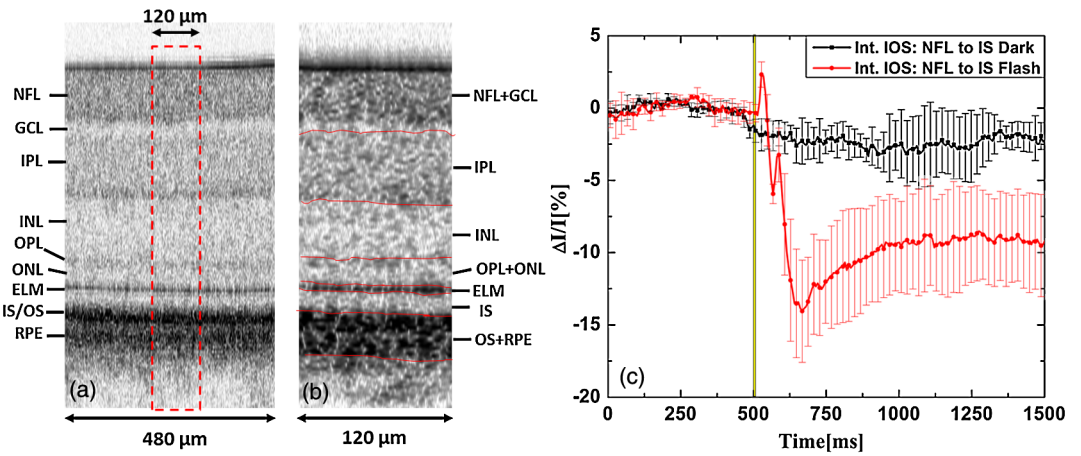

Fig. 1 Morphological image of the chicken retina (a) with selected region for IOS recordings (red line). Segmented fOCT tomogram (b). Representative, depth-integrated IOS traces (c) corresponding to "single-flash" (red line) and "dark" scans (black line). The yellow line marks the timing and duration of the visual stimulus.

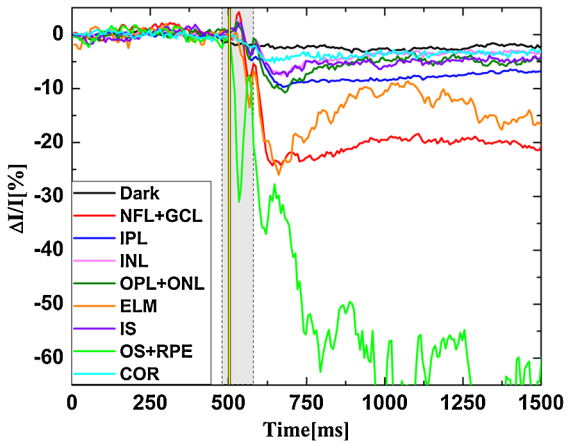

Fig. 2 Representative IOSs recorded from all segmented retinal layers. The gray area marks the ∼100-ms region over which the fast visually evoked IOSs develop in all retinal layers. The yellow line marks the timing and duration of the visual stimulus.

the recording (slow IOSs). Note that the OS-RPE trace in Fig. 2 was reduced in magnitude by five times. For comparison, no reflectivity changes were observed in all retinal layers during a "dark scan," or in the choroid in a "single-flash" scan during first 100 ms after the stimulus on-set. This suggests that the IOS measured in all retinal layers in "single flash" fOCT recordings are evoked by the visual stimulus. The IOS traces from all retinal layers except for the OS-RPE layer show a sharp decrease in the reflectivity at $t = 600$ ms from the start of the fOCT recording and a slow recovery to a new baseline at $t = 1,000$ ms. Very similar behavior was observed in the choroid IOS trace, which suggests that this effect may not be a visually evoked functional retinal response. Considering that the diameter of the fOCT imaging beam is 2.5 mm at the cornea and the diameter of the naturally dark dilated chicken pupil was between 3 and 3.5 mm, it is likely that the observed slow changes in the retinal layer reflectivity are due to vignetting of the imaging beam resulting from stimulus-induced pupil constriction and subsequent dilation. According to previously published research,[19–21] visually evoked pupil constriction in chickens begins ∼100 ms after the stimulus onset and occurs more rapidly than the subsequent dilation. The pupil dynamics timing and behavior described by Barbur et al.[21] match well with the changes observed in the slow IOSs from the choroid (pale blue line in Fig. 2) and all retinal layers (except for the OS-RPE layer) for the $t = 600$ ms to ∼1,000 ms from the start of the fOCT recording; therefore, it is very likely that the slow IOS changes are due to pupil-induced vignetting of the fOCT imaging beam. The IOS measured from the OS-RPE layer showed very strong oscillations in tissue reflectivity during the same time period. This suggests that the IOS measured in the OS-RPE layer is most likely a convolution of stimulus-induced changes in the tissue reflectivity associated with post-flash recovery processes in the photoreceptors and RPE cells, which can last up to a few hundred milliseconds after stimulus onset,[1] and pupil-induced vignetting of the fOCT imaging beam.

Figure 3 shows a magnified view of the gray area in Fig. 2 and presents a comparison between the fast IOSs (mean of six "single flash" recordings) and the simultaneously recorded ERG traces. Figure 3(a) shows that the a-wave (the negative peak of the ERG trace) appears ∼15 ms after the visual stimulus onset, which correlates well with previous ERG studies in living chicken retina and indicates normal photoreceptor function.[19,20] The corresponding IOSs measured in the inner retinal layers, from the NFL to the ONL, show very small (∼1% to 5%) positive changes and peak between 27 ms and 33 ms post-flash onset, which appear to correlate with the end of the steep rise of the b-wave (the positive peak in the ERG recording). Furthermore, these IOSs show a subsequent decrease in reflectivity, with minima between 67 ms and 73 ms after stimulus onset for the individual inner retinal layers. The negative

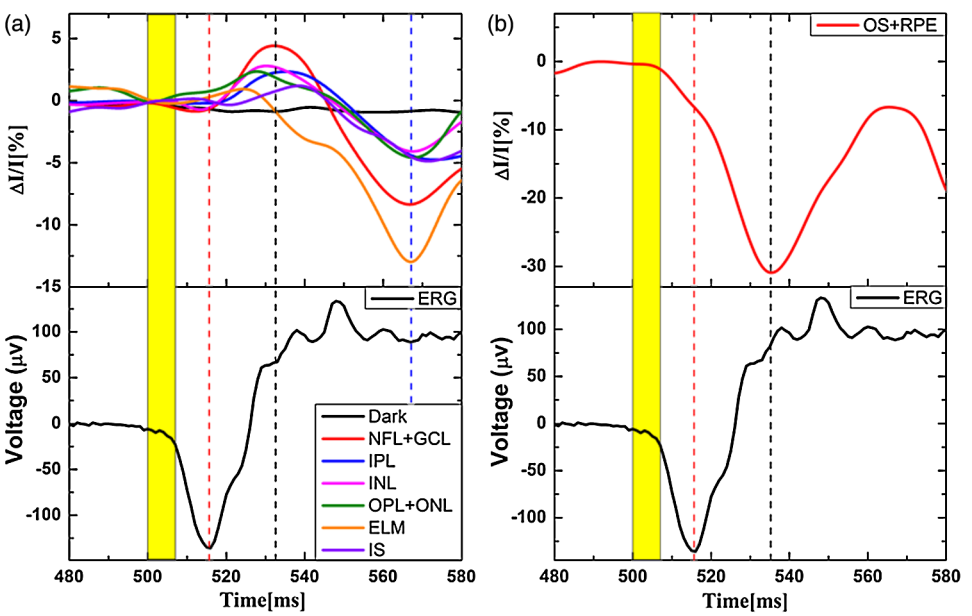

Fig. 3 Comparison of the visually evoked IOSs (mean of six measurements, top row) and ERG traces (bottom row). Individual IOSs recorded in all segmented layers (a), IOSs recorded in the OS-RPE layer (b), and integrated IOSs from the NFL to the IS (c). The time scale corresponds to the gray area marked in Fig. 2. The yellow line marks the timing and duration of the visual stimulus.

peaks in the IOSs correlate well with the end of the oscillatory potentials in the ERG recordings.

Fig. 3(b) shows a comparison between the IOSs recorded from the OS-RPE layer and the ERG trace. The OS-RPE trace shows a slow decrease in tissue reflectivity between 5 ms and ∼15 ms after stimulus onset, a subsequent faster decrease, and a negative peak at 34 ms after stimulus on-set. This behavior was followed by a fast increase in reflectivity, which peaked at 67 ms after stimulus onset. The negative peak in the OS-RPE IOS appears to correlate with the end of the steep rise of the B-wave and the positive peak in the IOSs recorded from the inner retinal layers, whereas the positive peak appears to correlate with the end of the oscillatory potentials in the ERG and the negative peak in the IOSs measured in the inner retinal layers. Considering the fact that the ERG trace is an integrated electrical response of different retinal cells comprising the retinal layers, it is likely that the difference between the timing of the positive and negative peaks in the IOSs from various retinal layers and the a- and b-waves in the ERG trace is due to a combination of the electrical responses that occur simultaneously in different retinal layers. For example, the slow PIII response, the cornea-negative wave potential that is maintained for the duration of the light flash in the ERG recording, is masked by the simultaneous positive electrical activity in the inner retina arising from the bipolar and Müller cells, thus defining the timing and magnitude of the a- and b-wave peaks.[1] In contrast, fOCT measures the individual optical responses from the various retinal layers that correspond to physiological processes such as cell membrane de- or hyperpolarization, cell swelling or deswelling resulting from ion exchange and water in- and efflux between the intra- and extracellular matrix, metabolic activity, etc. Although these physiological processes develop in parallel over time, fOCT in contrast to ERG, is able to resolve the spatial location in the retina (in depth) where these processes occur.

4 Discussion

Although in this paper we have presented multiple recordings from only one chicken, very similar responses were recorded repeatedly in the retinas of all five chickens used in this study. The timing of the negative and positive peaks of the fast IOSs recorded from different retinal layers was consistently within 10% of the values measured from the recordings presented in Figs. 2 and 3. However, the IOS magnitude varied significantly (> 50% for some retinal layers) for recordings acquired from the individual chicken used in this study. This variability could be attributable to a number of factors, such as the health status of each bird and its reaction to the anesthesia, the optical clarity of the eye, which is strongly dependent on the previous two factors, etc. More extensive studies of a significantly larger number of birds are required to establish the exact causes and statistical significance of the variability of the IOS magnitude.

To evaluate the spatiotemporal variation of the visually evoked IOSs measured in individual retinal layers, $x - y$ cross-sections from the 3D image stack were selected. Figure 4 shows the spatio-temporal profiles obtained from the NFL-GCL layer [Fig. 4(a)] and the OS-RPE layer [Fig. 4(b)], as well as the

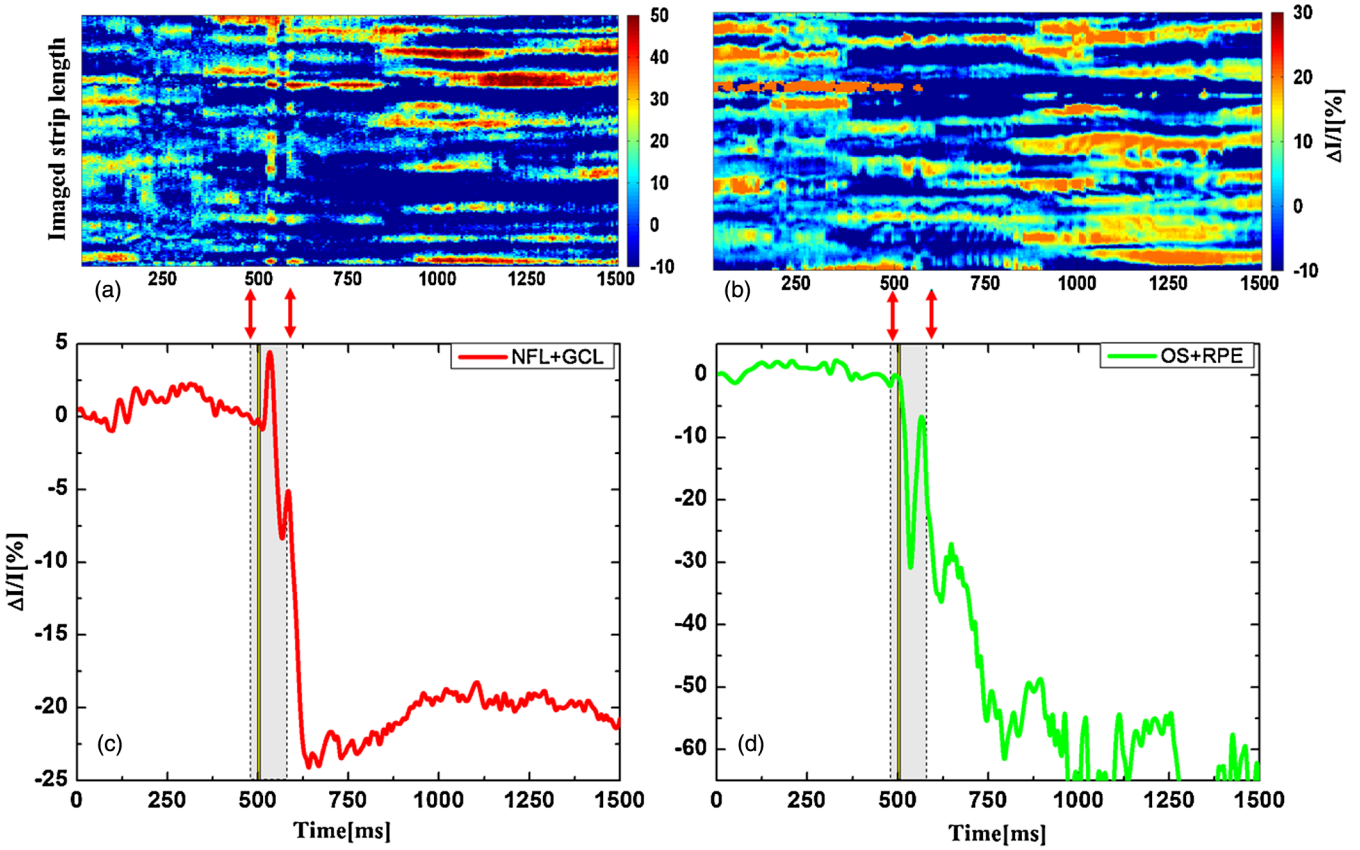

Fig. 4 Spatiotemporal profiles of the IOSs measured in the NFL-GCL layer (a) and the OS-RPE layer (b), as well as corresponding IOS trace averages for these layers.

corresponding IOS traces [Figs. 4(c) and (d)] for those layers obtained by averaging the pixel intensity from the spatio-temporal images over the length of the imaged strip [vertical axes in Figs. 4(a) and (b)]. The red arrows and the pale gray rectangles in Figs. 4(c) and (d) mark the 100 ms region of interest, similar to the one shown in Fig. 2. Although the two spatiotemporal profiles show significant variation with time and lateral spatial location in the retina, they also show clear negative and positive responses within ~100 ms from the application of the visual stimulus that become distinct peaks in the average traces. Considering the very small size of the retinal volume that was sampled in this study (~5 μm × 120 μm × retinal thickness) and the typical size of retinal cells, it is difficult to determine a clear relationship between the observed spatiotemporal profiles of the IOSs measured in individual retinal layers and visually evoked physiological processes that occurred in those layers. Future advances in fOCT technology that enable faster scanning of larger retinal volumes while preserving high temporal resolution would allow for the exploration of such a relationship.

The fOCT results presented here appear to correlate well with the results of previously published studies. For example, a fast visually evoked increase in the tissue reflectivity of the GCL and the inner nuclear layer (INL), as well as a simultaneous decrease in the photoreceptor layer reflectivity, was reported by Yao and Zhao [10] for *ex vivo* studies of the leopard frog. The timing of the positive and negative peaks for these retinal layers appears very similar to the results presented in our present paper. Differences in the magnitude of the measured IOSs can be attributed to differences in the imaging techniques used (near-infrared microscopy used by Yao vs. fOCT used in our study), the animal models used (frog vs. chicken retina), and the measurement conditions (*ex vivo vs. in vivo*). The fast negative IOSs measured in the OS-RPE layers in our studies also appear to correlate very well with a decrease in human cone reflectivity measured in the outer segment of individual retinal cones *in vivo* with adaptive optics,[9] which peaks at ~36 ms after stimulus onset (compared to 34 ms measured in the chicken retina in this study). Because authors of other published *in vivo* animal[14] and human fOCT studies[15,16] reported slow IOSs measured with time resolution >100 ms, IOSs in the literature cannot be compared directly with the fast retinal IOSs measured in our study.

Considering the complex physiology of the living retina, further thorough studies are required to investigate the physiological origins of retinal visually evoked IOSs. The imaging procedures and apparatus described here could be adapted in the future for non-invasive functional imaging of the human retina. A significant obstacle in such studies will be the proper management of any eye motion-related imaging artefacts that could mask the small-magnitude IOSs in some retinal layers.

5 Conclusions

In summary, fast visually evoked IOSs were recorded noninvasively and *in vivo* in all individual layers of the chicken retina with a combined fOCT-ERG system. The IOSs showed clear correlation with ERG traces acquired simultaneously. The ability to record visually evoked signals from individual cell layers in the retina non-invasively and *in vivo* could improve the understanding of how retinal cells communicate with each other and respond to external stimuli in healthy and diseased retinas.

Acknowledgments

The authors thank K. Dworski and H. van der Heide for assistance with the electrical and mechanical design of the fOCT system, and N. Gibson with assistance with the chicken management. This work was supported by a research grant from the Natural Sciences and Engineering Research Council of Canada and in-kind contributions from Diagnosys LLC.

References

1. J. R. Heckenlively and G. B. Arden, *Principles and Practice of Clinical Electrophysiology of Vision*, 2nd ed., MIT Press, Cambridge, MA (2006).
2. A. Grinvald et al., "Optical imaging of neuronal activity," *Physiol. Rev.* **68**(4), 1285–1366 (1988).
3. A. Villringer and B. Chance, "Non-invasive optical spectroscopy and imaging of human brain function," *Trends Neurosci.* **20**(10), 435–442 (1997).
4. M. A. Duarte et al., "Functional imaging of the retinal layers by laser scattering: an approach for the study of Leaõ's spreading depression in intact tissue," *J. Neurosci. Methods.* **123**(2), 139–151 (2003).
5. M. D. Abràmoff et al., "Visual stimulus-induced changes in human near-infrared fundus reflectance," *Invest. Opthamol. Vis. Sci.* **47**(2), 715–721 (2006).
6. K. Tsunoda et al., "Mapping cone- and rod-induced retinal responsiveness in macaque retina by optical imaging," *Invest. Ophthalmol. Vis. Sci.* **45**(10), 3820–3826 (2004).
7. R. S. Jonnal et al., "In vivo functional retinal imaging of human cone photoreceptors," *Opt. Express.* **15**(24), 16141–16160 (2007).
8. K. Grieve and A. Roorda, "Intrinsic signals from human cone photoreceptors," *Invest. Ophthalmol. Vis. Sci.* **49**(2), 713–719 (2008).
9. J. Rha et al., "Variable optical activation of human cone photoreceptors visualized using a short coherence light source," *Opt. Lett.* **34**(24), 3782–3784 (2009).
10. X. C. Yao and Y. B. Zhao, "Optical dissection of stimulus-evoked retinal activation," *Opt. Express.* **16**(17), 12446–12459 (2008).
11. W. Drexler and J. G. Fujimoto, "State-of-the-art retinal optical coherence tomography," *Prog. Retin. Eye Res.* **27**(1), 45–88 (2008).
12. X. C. Yao et al., "Rapid optical coherence tomography and recording functional scattering changes from activated frog retina," *Appl. Opt.* **44**(11), 2019–2023 (2005).
13. K. Bizheva et al., "Optophysiology: depth-resolved probing of retinal physiology with functional ultrahigh-resolution optical coherence tomography," *Proc. Natl. Acad. Sci. U.S.A.* **103**(13), 5066–5071 (2006).
14. V. J. Srinivasan et al., "In vivo measurement of retinal physiology with high-speed ultrahigh resolution optical coherence tomography," *Opt. Lett.* **31**(15), 2308–2310 (2006).
15. A. R. Tumlinson et al., "Techniques for extraction of depth-resolved in vivo human retinal intrinsic optical signals with optical coherence tomography," *Jpn. J. Ophthalmol.* **53**(4), 315–326 (2009).
16. V. J. Srinivasan et al., "In vivo functional imaging of intrinsic scattering changes in the human retina with high-speed ultrahigh resolution OCT," *Opt. Express.* **17**(5), 3861–3877 (2009).
17. T. Schmall, C. Kolbitsch, and R. A. Leitgeb, "In vivo functional retinal optical coherence tomography," *J. Biomed. Opt.* **15**(4), 041513 (2010).
18. A. A. Moayed et al., "In vivo imaging of intrinsic optical signals in chicken retina with functional optical coherence tomography, " *Opt. Lett.* **36**(23), 4575–4577 (2011).
19. J. Rymer et al., "The albino chick as a model for studying ocular developmental anomalies, including refractive errors, associated with albinism," *Exp. Eye Res.* **85**(4), 431–442 (2007).
20. J. M. McGoogan and V. M. Cassone, "Circadian regulation of chick electroretinogram: effects of pinealectomy and exogenous melatonin," *Am. J. Physiol. Regul. Integr. Comp. Physiol.* **277**(5), R1418–R1427 (1999).
21. J. Barbur et al., "A comparative study of stimulus-specific pupil responses in the domestic fowl (*Gallus gallus domesticus*) and the human," *Vision Res.* **42**(2), 249–255 (2002).